Journal of Polymer Research (2021) 28: 154
https://doi.org/10.1007/s10965-021-02516-y

ORIGINAL PAPER

Nanocomposite synthesis of silver doped magnesium oxide incorporated in PVC matrix for photocatalytic applications

Nouhad Rouabah[1] · Boubekeur Boudine[2] · Roshan Nazir[3] · Mourad Zaabat[1] · Ali S Alqahtani[4] · Mohammed S Alqahtani[5] · Rabbani Syed[5]

Received: 22 January 2021 / Accepted: 29 March 2021 / Published online: 8 April 2021

Abstract

This work reveals a sol–gel approach for synthesis of silver doped magnesium oxide (Ag:MgO) incorporated in PVC matrix to give Ag:MgO/PVC nanocomposite. On glass substrate three different percentages of Ag:MgO/PVC (3,7, and 10%) were deposited by spin coating method. This film of Ag:MgO/PVC nanocomposites were characterized using AFM, UV–Vis, XRD and FTIR analysis. The results of XRD revealed the formation of Ag doped MgO nanoparticles with two phases (MgO and metallic Ag) in the matrix of PVC with the average size of nanoparticles equal to 31.5,22.29, 23.77, 29.68 nm. The direct band gap energy for PVC and pure MgO/PVC was 4.1 eV and 3.85 eV respectively. The band gap energy value changes from 3.85 eV, 3.75 eV, 3.71 eV, 3.69 eV with increasing Ag:MgO concentration(3–10%). Atomic force microscopyalso shows a change in the roughness of the nanocomposites film with increasing Ag:MgO nanoparticles percentage. The photocatalytic activity of this nanocomposite film was evaluated for the methylene blue (MB) dye under UV light irradiation. The result demonstrated good potential of Ag:MgO/PVC nanocomposites films for MB degradation with a suitable photocatalytic reaction proposed mechanism. The kinetic studies revealed a rate constant of 6.25×10^{-3} min^{-1} for 10% Ag:MgO/PVC nanocomposite thin films.

Keywords MgO nanoparticles · Sol–gel · Polyvinyl chloride PVC · Photocatalysis

Introduction

Nanocomposites embedded in polymer matrix have gained a lot of interest and thus a numerous research workhas been devoted to it. Single polymer matrix is one of the most attractive classes of materials in the world, due to their interested properties and applications. Polymer nanocomposites offer advanced in new technology in various uses and has no environmental benign effects. Moreover, the effective properties of polymer nanocomposites rely on the nature of the components, the shape of the particles, the size and arrangement of the inclusions, the concentration, the volume fraction of the components, extent of dispersion of nanoparticles and interfacial bonding in the polymer matrix. Generally, Inorganic particles in polymer matrix improve density, mechanical, thermal, electronic, magnetic, and redox properties of nanocomposites [1–4]. Among oxides, MgO nanoparticles is a well known refractory oxide, which has potential advantages with wide bandgap around 7.8 eV. MgO is interesting inorganic substance which has FCC type crystal packing, abundantly used raw material because of its high thermal stability, biodegradability and low toxicity. MgO is a chosen material due it's potential application in chemical industry as it is used as air pollutant scrubber for gases, catalysis, optoelectronics, insulating material filler, refractory materials, and as a catalyst support [5, 6]. In photocatalytic application MgO is seen one of the promising photocatalyst and have been successfully applied for methylene blue

✉ Nouhad Rouabah
nouhadrouabeh@gmail.com

1 Laboratoire Des Composants Actifs Et Matériaux, Université Larbi Ben, M'Hidi, Oum El Bouaghi, Algeria

2 Laboratoire de Cristallographie, Université des frères Mentouri, Constantine 1, Algeria

3 Department of Chemistry, Bilkent University, 06800 Bilkent, Ankara, Turkey

4 Department of Pharmacognosy, College of Pharmacy, King Saud University, P.O. Box 2457, Riyadh 11451, Saudi Arabia

5 Department of Pharmaceutics, College of Pharmacy, King Saud University, PO Box 2457, Riyadh 11451, Saudi Arabia

dye degradation. Doping of MgO is an effective method to increase photocatalytic activity of MgO catalyst. Reports have revealed insertion of silver nanoparticles in the crystal lattice of MgO enhance the photocatalytic activity for dye degradation. [7] The doping of Ag results in lower energy region absorption of light and thus makes possible to extend the photocatalysis in the visible part of electromagnetic spectrum. Polymers are the dominant materials widely used, owing to their low cost and ease of processing, so they are considered to be versatile, beneficial and economical for their wide spread applications. [8] Polymers like PVC has attained tremendous interest in various life aspects. The interest in PVC have arisen because of its good properties like excellent mechanical properties, highly rigidity than other general thermoplastics materials. The advantage of PVC is that it breaks down easily and does not produce dioxins under natural conditions. PVC also has find good applications in antibacterial and industries. [9, 10]

In this work, an attempt has been made to synthesized Ag doped MgO nanoparticles and Ag doped MgO/PVC nanocomposites and investigate their photocatalytic activity. we have also given well full details about the structural, optical, and morphological properties of Ag:MgO/PVC nanocomposites film.

Experimental section

Synthesis of magnesium oxide (MgO) nanoparticles (NPs)

A sol–gel technique was employed to synthesize MgO NPs. Mg $(NO3)_2.6H_2O$ was taken as a precursor of magnesium and treated with C_2H_5OH. The solution was stirred for 24 h until white gel was obtained. After that the mixture was filtered, washed with distilled water and ethanol several times and dried at 100° C for 24 h.Theobtained powder was annealed at 950° C for 36 h. Finally the powder was grinded and used for further analysis. The annealing phase results in formation of desired product.

Synthesis of Ag-doped MgONPs: Same sol–gel technique was employed to synthesize Ag-doped MgO NPs. In brief, In 20 ml di-ionized (DI) water 0.019 mol $Mg(NO_3)_2{\cdot}6H_2O$ and X mol (X = 0.001, 0.002, 0.003) of $AgNO_3$was mixed followed by addition of 0.02 mol of $C_6H_8O_7{\cdot}H_2O$ under constant stirring for 2 h. Subsequently the mixture was kept on a water bath at 80 °C until a wet gel formed. After that wet gel was dried at 150 °C to form a fluffy precursor. Finally, the precursor was grinded and calcined at 600 °C in presence of air for 2 h at a heating rate of 2 °C/min.

Ag:MgO/PVC nanocomposites preparation of polymer nanocomposites:

Ag:MgO/PVC nanocomposites was fabricated by adding 1 g of PVC powder in 20 ml THF for 30 min and a clear transparent viscous solution was obtained. A selected amount of Ag: MgO (depends upon loading taken) was added in 10 ml of THF and mixed to PVC solution under constant stirring for 1 h. The weight of Ag: MgO added to polymer solution depends upon the different percentage by weight 3%, 7%, 10% Ag:MgO/PVC. After that the solution was allowed to rest which resulted in deposition of heavier particles to get settle at the bottom and the smallest crystallites in the upper part were recovered and deposited as Ag:MgO/PVC nanocomposite thin film on the surface of the glass. Before depositing the film the glass was cleaned and washed by using DI water, methanol and acetone in order to remove the unwanted things (grease and other impurities). Spin coating or centrifugation technique was used to deposit Ag:MgO/PVC nanocomposite on glass substrate. After deposition the thin film was completely dried in order to remove traces of solvents. As synthesized film was having uniform distribution of Ag:MgO NPs.

Photocatalytic procedure

A UV light source (VL -215.LC, 15 W), with emission maximum at 365 nm was employed to check the photocatalytic activity of Ag:MgO/PVC. 10 ml MB solution with an initial concentration of 10^{-5} mg/ml was taken in a glass beaker. A thin glass strip (5 × 2.5 cm) containing the films of Ag:MgO/PVC nanocomposites was put in the beaker containing MB. The beaker was kept undervisible light at a distance 20 cm emitted by a 300 W iodine tungsten lamp (Philips and Co). The whole system was covered by cloth so that natural white light would have no role in catalysis. During irradiation the aliquots of solution was taken out after every 30 min fromthe reactor and checked by analyzed by a 723 UV–Vis spectrometer (UV-1800 Shimadzu LC 2010-HT).

Results and discussion

Structural study

X-ray diffraction (XRD) analysis

Figure 1 shows the XRD patterns of pure PVC, MgO/PVC and Ag:MgO/PVC nanocomposites film of different concentration (3, 7 and 10) wt% of Ag doped MgO nanopowder under study. From, XRD of pure PVC film, polymer chain have disordered structure indicating amorphous nature [11,

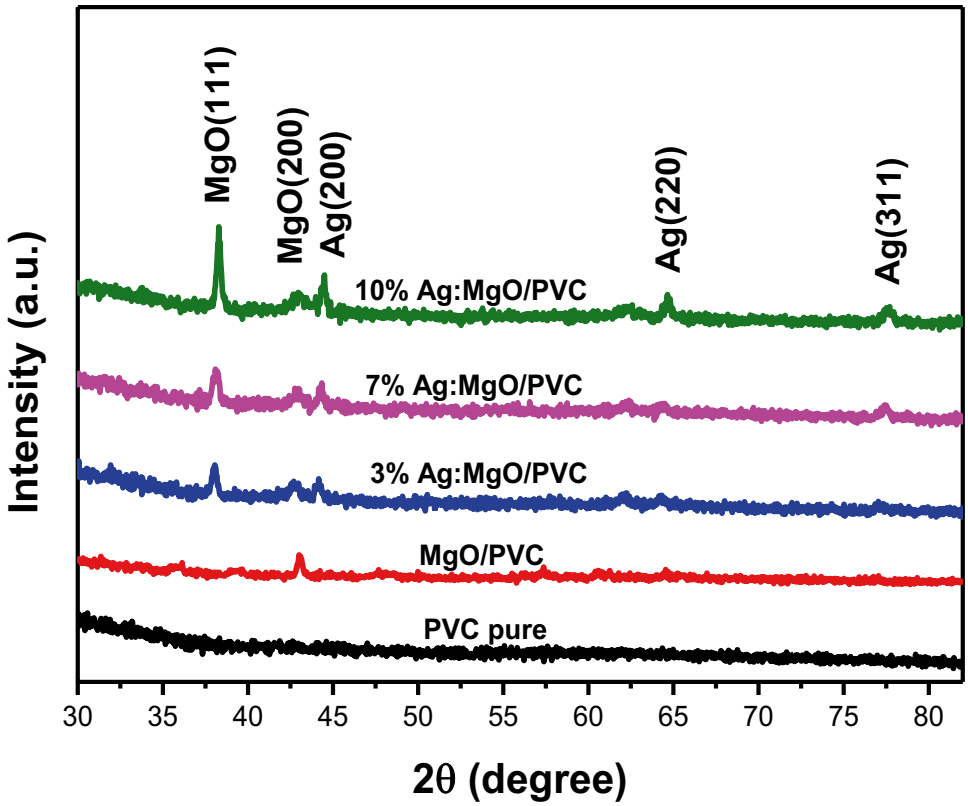

Fig. 1 X-ray diffraction spectra of Pure PVC, MgO/PVC and Ag:MgO/PVC nanocomposites thin films

12]. The MgO/PVC nanocomposites film exhibits lower characteristic peaks as compared to the Ag:MgO/PVC nanocomposites, which appear the peak at 2θ angle 36.23°, 43.04° corresponding to the reflection of of (111) and (200) correspond to the cubic phase of MgO (JCPDS card N° 45–0946). The prominent (111) peak of MgO exists but very less intense. The XRD pattern of 3% Ag:MgO/PVC reveals MgO crystalline phase and no prominent peak for Ag. However when the amount of Ag:MgO is higher(7%,10%), a notable intense peak is observed at 2θ = 38.11° that arises due to diffraction of metallic Ag [7]. The appearance of these three additional peaks at 44.5°, 64.72° and 77.65° corresponds to the (200),(220) and (311) planes of metallic Ag, authenticates presence of metallic Ag as second phase crystal planes in the polymer matrix, which indicates the successful insertion of elemental silver on MgO/PVC nanocomposites [13]. From Table 1 it can be inferred that intensity and area of Ag:MgO/PVC under the peaks at 2θ = 39.3° and 43.04° shifts to right when Ag:MgO loading is increased as compared with that of MgO/PVC, this decrease in lattice parameters reflects formation of mixed phase of Ag:MgO. So it can be inferred that there is change in crystal structure due to varying of Ag:MgO dopant ratio. The interplaner distance (d) of MgO/PVC and Ag:MgO/PVC were determined using Bragg's law. The change in the interplaner distance (d) from 2.29 for MgO/PVC (0% Ag) to 2.36 for highest loading of Ag:MgO (10 at.% Ag:MgO) clearly indicates the increase in the lattice size upon doping, which demonstrating a possible extension of MgO lattice due to substitution of larger Ag^{+} ions (1.26 Å) with the Mg^{2+} (0.66 Å) ions in the lattice. In this process oxygen vacancies are also generated

Table 1 Structural parameters MgO/PVC and Ag: MgO/PVC nanocomposites thin films

Samples	2θ(°)	(hkl)	FWMH (rad)	d	D (nm)
MgO/PVC	43,08	(200)	0,27	2,10	31,5
3%Ag:MgO/PVC	38,03	(111)	0,4	2,35	22,29
	42,72	(200)	0,35	2,05	
	44,17	(200)	0,4	2,05	
7% Ag:MgO/PVC	38,16	(111)	0,35	2,35	23,77
	42,94	(200)	0,48	2,04	
	44,3	(200)	0,4	2,04	
	77,35	(311)	0,31	1,23	
10% Ag:MgO/PVC	38,3	(111)	0,28	2,36	29,68
	42,94	(200)	0,48	2,04	
	44,43	(200)	0,3	2,04	
	64,72	(220)	0,3	1,44	
	77,65	(311)	0,3	1,23	
	42,94	(200)	0,48	2,04	
	44,43	(200)	0,3	2,04	
	64,72	(220)	0,3	1,44	
	77,65	(311)	0,3	1,23	

to favour the structure reorganization and keep an overall neutral charge after Mg^{2+} in MgO crystal is replaced by Ag^{+} [14]. Additionally to these observations, after doping with Ag, the peak of (111) has a high intensity value. Compared to the JCPDS card N° 45–0946, MgO present a texture along the (111) plane. Zhou et al., revealed that the (002) peak of Ag-doped ZnO film first shifted to a lower angle and then shifted back to a higher angle with increasing Ag addition [14]. Kang et al. deemed that the shift of the (002) peak was closely related to the lattice sites of Ag in ZnO [15]. With the increase of Ag addition, the lattice parameters of ZnO increase from 5.225 to5.270 Å, and then decrease to 5.241 Å. it is found that the c values (of the c-axis of ZO films) are larger than that of standard data (c_o -5.205 Å). This suggests that the peak shift ought to be due to the different degree of increase of the lattice constant in c-axis direction caused by a different degree of substitution of Zn^{2+} ions by Ag^{+} ions. For Ag-doped further increased c values, Li et al. reported that an in-crease has been determined when Zn^{2+} ions are replaced by Ag^{+} ions because of the larger radius of Ag^{+} ions (1.26 Å) than Zn^{2+} ions (0.74 Å) [16]. The increase in the parameters of the c-axis can be caused by either interstitial incorporation of Ag ions into the lattice or Ag ions substitution of the Zn ion [. 14]. This proves that the Ag ions have been incorporated into the ZnO lattice successfully. In our case we believe there is also possible extension of MnO lattice due to substitution of larger Ag^{+} ions (1.26 Å) with the Mg^{2+} (0.66 Å) ions in the lattice. Similar to Ag-doped ZnO film the size of Ag^{+} ions (1.26 Å) with the Mg^{2+} (0.66 Å) in silver doped magnesium oxide is comparable to size of Ag and Mg in Ag-doped ZnO. Ag ions in MgO lattice behave as monovalent dopant ions which have the ability to occupy both the lattices and interstitial sites.

According to Cai and Coworkers (17) when Ag is doped into MgO lattice, Ag atom will occupy substitutional site rather than interstitial site since the radius of Ag^{+} (0.126 nm) is larger than that of Mg^{2+} (0.066 nm) [17]. Accordingly, oxygen vacancies will be generated to favour the structure reorganization and keep an overall neutral charge after Mg^{2+} in MgO crystal is replaced by Ag^{+}. The defect reaction equation can be expressed as follows:

$$Ag_2 \xrightarrow{O2MgO} 2Ag *_{Mg} + Vo + Oo$$

The grains size

Debye Scherer's formula was used to calculate size of crystals [18], and the values calculated are recorded in Table 1:

$$D = \frac{0.9\lambda}{\beta cos\theta} \quad (1)$$

where β = FWHM, θ is the diffraction angle, λ is the X-ray wavelength (1.5405 Å). As the dopant Ag:MgO increases the for Ag:MgO/PVC samples the crystallite size (D) also increases.

FTIR analysis

In the range of 4000–400 $cm^{-1}$of the FTIR spectra of pure PVC, PVC/MgO and Ag:MgO/PVC nanocomposits films were recorded as shown in Fig. 2. Sharp peak were recorded in the all films at 756 and 904 cm^{-1}. This was attributed to the PVC Bond. With the increase in Ag:MgO loading there is a clear shift towards lower frequencies indicating Ag doped MgO interactions with C–Cl, C-H bonds of PVC. matrix, due to interaction between Ag doped MgO and C–Cl, C-H bonds of PVC. [19] The spectrum of MgO/PVC nanocomposites film appears three distinct band is observed in the wave number 615, 1324,1434 cm^{-1}, indicating the bending vibrations of Mg–O–Mg, C-H and C = C,respectively. [20] The spectrum of the Ag: MgO / PVC nanocomposite film displayed at the low frequencies of 485 cm^{-1} and 2360 cm^{-1} were assigned to to the typical stretching mode of the Ag–O bond and the CH_2 bending vibration mode [21].

Optical study

UV–Vis analysis

To determine the optical properties of Ag:MgO/PVC nanocomposite thin film UV–Vis Spectroscopy was employed. The UV–VIS absorbance spectra in the region 200–800 nm for doped and undoped films are shown in Fig. 3, the pure PVC is completely fully transparent (90%) and has a steep

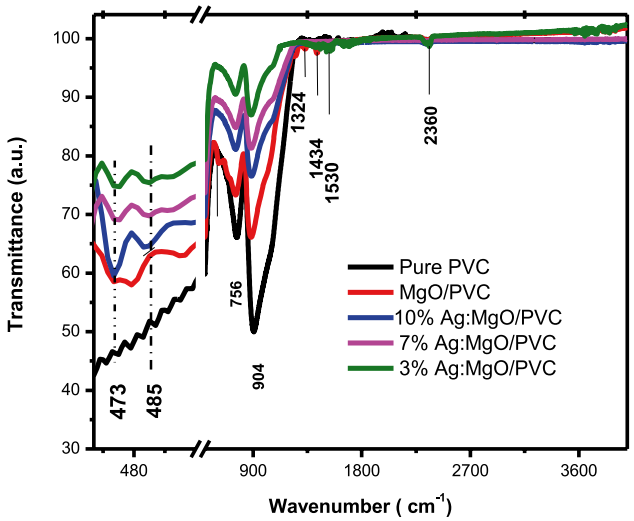

Fig. 2 FTIR spectrum of PVC, PVC/MgO and Ag:MgO/PVC nanocomposits

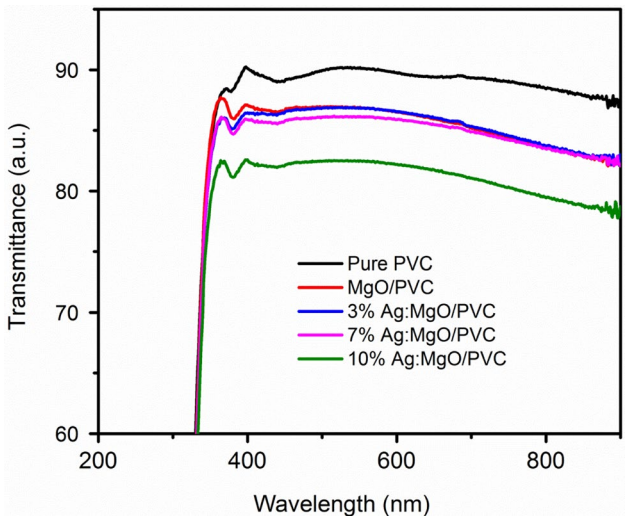

Fig. 3 Optical transmission spectra in the UV–Visible region of Pure PVC, MgO/PVC and Ag:MgO/PVC nanocomposites thin films

absorption edge at 300 nm. The absorption of the films gets decrease with the increase in Ag: MgO amounts concentration as shown in Fig. 3. The absorption region(300-400 nm) is probably due to electron transition from valence band to the conduction band. For Ag:MgO/PVC composite films this absorption band is quite prominent and wider than PVC pure and MgO/PVC. There is a slight shift in UV absorption intensity in Ag:MgO/PVC films. To obtain effective UV absorption the concentration of metal ions needs to be optimized as there is change in absorption with addition of Ag:MgO NPs in PVC matrix [22].

Determination of optical band

Tauc' plot method was employed to determine the optical band gap of PVC, MgO /PVC and Ag:MgO/PVC nanocomposites films. Using the classical Tauc approach, the band gap (Eg) was calculated fromthe plot of $(\alpha h\nu)^{1/2}$ vs. photon energy ($h\nu$), Fig. 4 shows direct optical band gap for neat PVC, MgO/PVC and Ag:MgO/PVC nanocomposites. The optical band gap for PVC was found ~ 4.1 eV. Incorporation of Ag-doped MgO has great influence on direct transition in nanocomposites as optical band gap gets decreased with increase in concentration of Ag-doped MgO nanoparticles. This is credited to formation of new local levels in the bottom of conduction band which aid in electron transport from valence band through local levels and then to conduction band [23]. These results revealed that the incorporation of PVC served as accepter for Ag:MgO which reduced the band gap (~ 3.69 eV) for 10% Ag:MgO/PVC nancomposite with red shift confirming p-type conductivity.

Morphological study

Atomic Force Microscopy (AFM) analysis

AFM is one of the important analyses for surface characterization. To investigate the topography and roughness of the thin films, AFM 3-D micrographs were recorded. This measurement technique presents digital images allow the quantitative measurements of roughness average, the root mean square and diameter of pores [24] and are estimated and tabulated below.

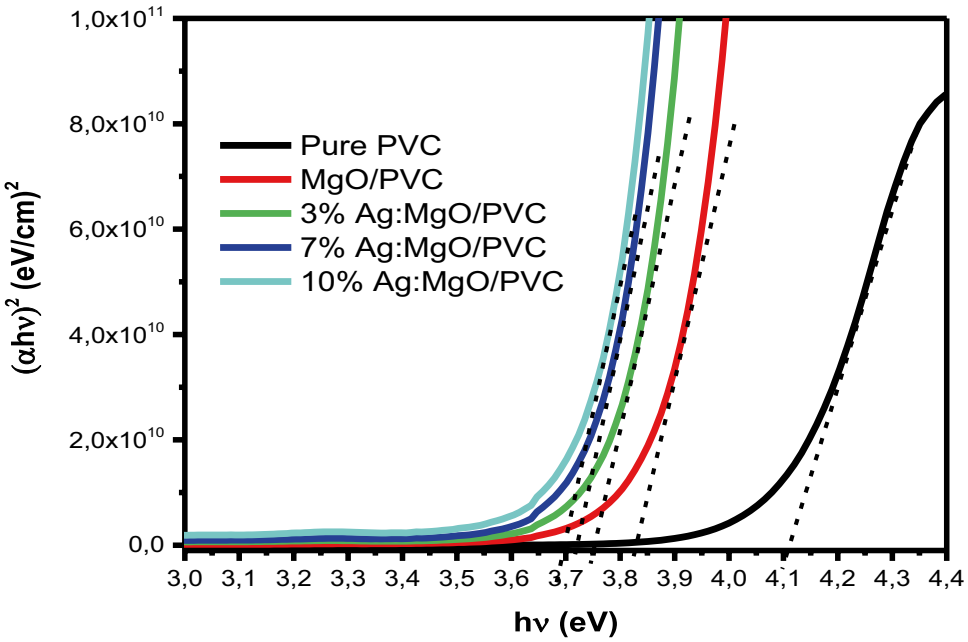

Fig. 4 The plot $(\alpha h\upsilon)^2$ versus incident energy ($h\upsilon$)

Table 2 Measurements of roughness average, the root mean square and diameter of pores of samples prepared

Samples	Avg. Diameter of pores	Roughness average	Root mean square
Pure PVC	36–360	1.93	4.12
PVC/MgO	31–500	34.07	42.30
PVC/MgO-Ag3%	25–500	28 0.49	734.76
PVC/MgO-Ag7%	12.5–375	31.33	837.29
PVC/MgO-Ag10%	31–375	35.59	644.64

The change in surface morphology and roughness due to incorporation of Ag doped MgO nanoparticles in PVC membranes is characterized. The mean roughness (Ra) and root mean square roughness (Rq) parameters were measured for these thin films and are displayed in Table 1 and Table 2. Both parameters increased with increase in the Ag:MgO doping weight percentage. It can be seen from Table 1 that mean roughness (Ra) is varied between $1.933 \leq Ra \leq 35.592$ and the root-mean squared roughness (Rq) is varied between $4.117 \leq Rq \leq 644.643$.It is clear that the RMS increased with Ag:MgO content, indicating that PVC/MgO-Ag nanocompositesfilms have a rougher surface than PVC/MgO nanocomposites.This is an acceptable concurrence with XRD results proposing a debasement of crystallinity and a huge change in MgO/PVC nanocomposites film microstructure. Appropriately, 7% and 10% Ag:MgO/PVC nanocomposites film has the most elevated permeable, which prompts a huge explicit surface region.Thusly, this permeable structure film most promising methods to improve the photocatalyst activity and make the recycling safety.

Figure 5 shows the two-dimensional and three-dimensional AFM images of the surface topography of PVC pure, MgO/PVC and Ag: MgO/PVC nanocomposits films of different concentrations. It can be seen that the number, diameter of the pores augment with increasing the Ag:MgO nanoparticles. may be due to the formation of agglomerates of nanosheets on the membrane surface during the phase

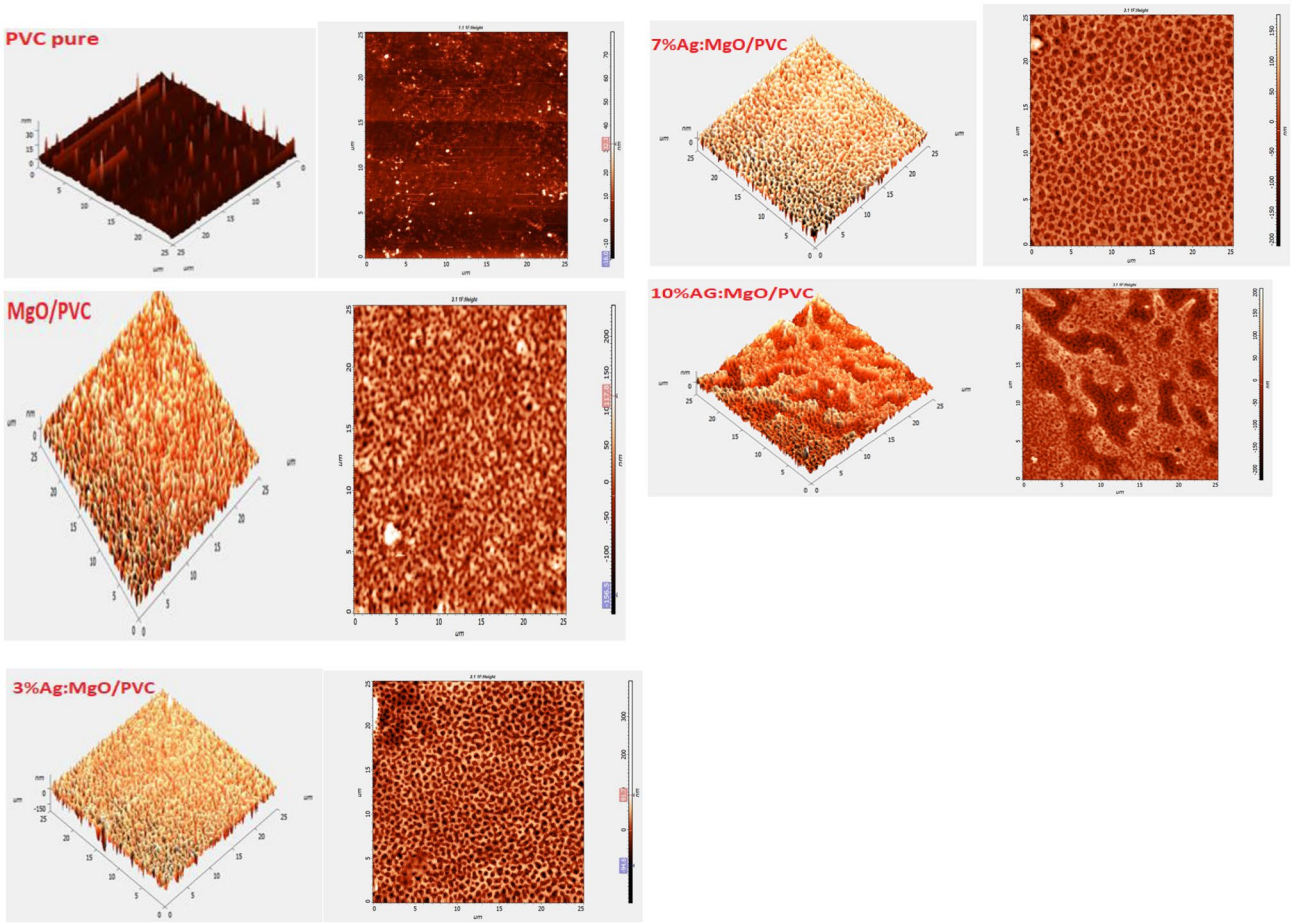

Fig. 5 AFM for pure PVC, PVC/MgO and Ag:MgO/PVC nanocomposits

inversion process. This is due to increase in the aggregation of tiny particles at some points that contributed in the increase in the roughness parameters [25]. As shown by AFM micrographs and their line profiles, 7%, 10% Ag:MgO/PVC nanocomposites films have high porous structure as compared to MgO/PVC. This indicates that Ag doping leads to an increased porosity and as a result leads to a large specific surface area.

Photocatalytic tests

The photocatalytic degradation of methylene blue by PVC pure, MgO/PVC and Ag:MgO/PVC nanocomposites are shown in the Fig. 6. The methylene blue degradation efficiency increases continuously with increases of time. After two hours of test period, the methylene blue degradation is found to be 17%, 32%,35%,46% and 52% for PVC,MgO/PVC and Ag:MgO/PVC with concentrations 3%,7%,10% respectively.Comparing pure PVC and Ag:MgO/PVC the highest activity is observed for the 10% Ag:MgO /PVC nanocomposites can be assigned to the most efficient charge separation. On the first hand, the presence of a proper content of silver can reduce electron–hole recombination and increase the photocatalytic activity. On the other hand, the introduced of Ag doped MgO onto the PVC matrix increases the rate of electron transfer to dissolved oxygen.

Figure 7 shows the kinetic plot between ln(C/C0) and irradiation time " t " for the photodegradation of methylene blue as a function of irradiation time for pure PVC,MgO/PVC and Ag doped MgO/PVCnanocomposites at different concentrations and a linear relationship is observed.The rate constant (k) was calculated from the slopes of PVC,MgO/PVC,(3%,7%,10%) Ag:MgO/PVC nanocomposites and it was found to be 1.64×10^{-3} min^{-1}, 3.31×10^{-3} min^{-1}, 3.50×10^{-3} min^{-1},4.24×10^{-3} min^{-1}, 6.25×10^{-3} min^{-1}, respectively. This shows that Ag:MgO/PVC has enhanced photo catalytic degradation than pure PVC. MgO /PVC has only a small effect on the MgO particle surface to reduce photocatalytic activity. In the case of Ag doped MgO, the photo catalytic activity increases due to the doping level has increased. This may be due to the highest porous structure, which provides more active sites for the adsorption of pollutant molecules. The diminution of the band gap (Eg) by the addition of Ag doped MgO in PVC matrix allow the absorption of more UV light energy and higher generation of electron–hole pairs [26]. This promotes the $\cdot OH$ and $O_2^{\cdot-}$ concentrations and thus improves the effectiveness of the photocatalyst. As a result, more electrons and holes can contribute in the photoreaction and so rise the removal of organic molecules [27].

Photodegradation mechanism

Photocatalytic degradation of Ag:MgO/PVC nanocomposites film is initiated by degradation of Ag doped MgO.Since the degradation of PVC starts indirectly through oxidative radicals generated on Ag doped MgO [28].

In general,when Ag doped MgO is irradiated by UV light, a photoelectron moves from valence band of the semi conductor and iel is the intermedite energy levels generated after doping process.This photon has the energy (hυ) equal to or greater than the band gap.The semi conductor absorbs this radiation and one electron can be excited from the doping donor level to Cb of the semi conductor and forms cationic radicals (eq(2)).

$$Ag:MgO+hu(E\geq E_g)\rightarrow Ag:MgO^{*}(e_{cb}^{-}+h_{vb}^{+}) \tag{2}$$

The photogenerated holes (h_{vb}^{+}) react with water molecules to produces the hydroxyl radicals $\cdot OH$. While the electrons in (CB) conduction band meanwhile reacts with O2 and generate superoxide radicals anions $O_2^{\cdot-}$(Eq. (3)). the oxygen molecules adsorbed on the semi conductor surface accelerates oxidation process and also prevent any further e- / holes recombination by trapping electrons.

$$h_{vb}^{+}+H_2O\rightarrow\cdot OH \tag{3}$$

$$e_{cb}^{-}+O2\rightarrow O_2^{\cdot-} \tag{4}$$

These reactive species like H2O2, $O_2^{\cdot-}$ and $\cdot OH$ radicals produced, for ultimately help to degrade target pollutants present around it (Eq. (5,6,7)).

$$O_2^{\cdot-}+H2O\rightarrow O_2^{\cdot}H+OH^{-} \tag{5}$$

$$2O_2^{\cdot}H\rightarrow H_2O_2+O_2 \tag{6}$$

$$H_2O_2+h\upsilon\rightarrow 2\cdot OH \tag{7}$$

Photocatalytic degradation of PVC is only excited by UV light due to presence of C–C and C-H bonds in polyvinyl chloride. It is proposed that in PVC/MgO nanocomposites, on MgO nanostructures-MB dye generates holes in ground state which takes part in degradation of PVC matrix also with $\cdot OH$and $O_2^{\cdot}H$. These oxygenated species are initiators of PVC degradation by attacking the polymeric chain.

$$-\left(CH_2CHCl\right)-*+\cdot OH\rightarrow(\cdot CHCHCI)-+H_2O \tag{8}$$

$$-(CH_2CHCl)-*+\cdot O_2H\rightarrow(\cdot CHCHCl)-+H_2O_2 \tag{9}$$

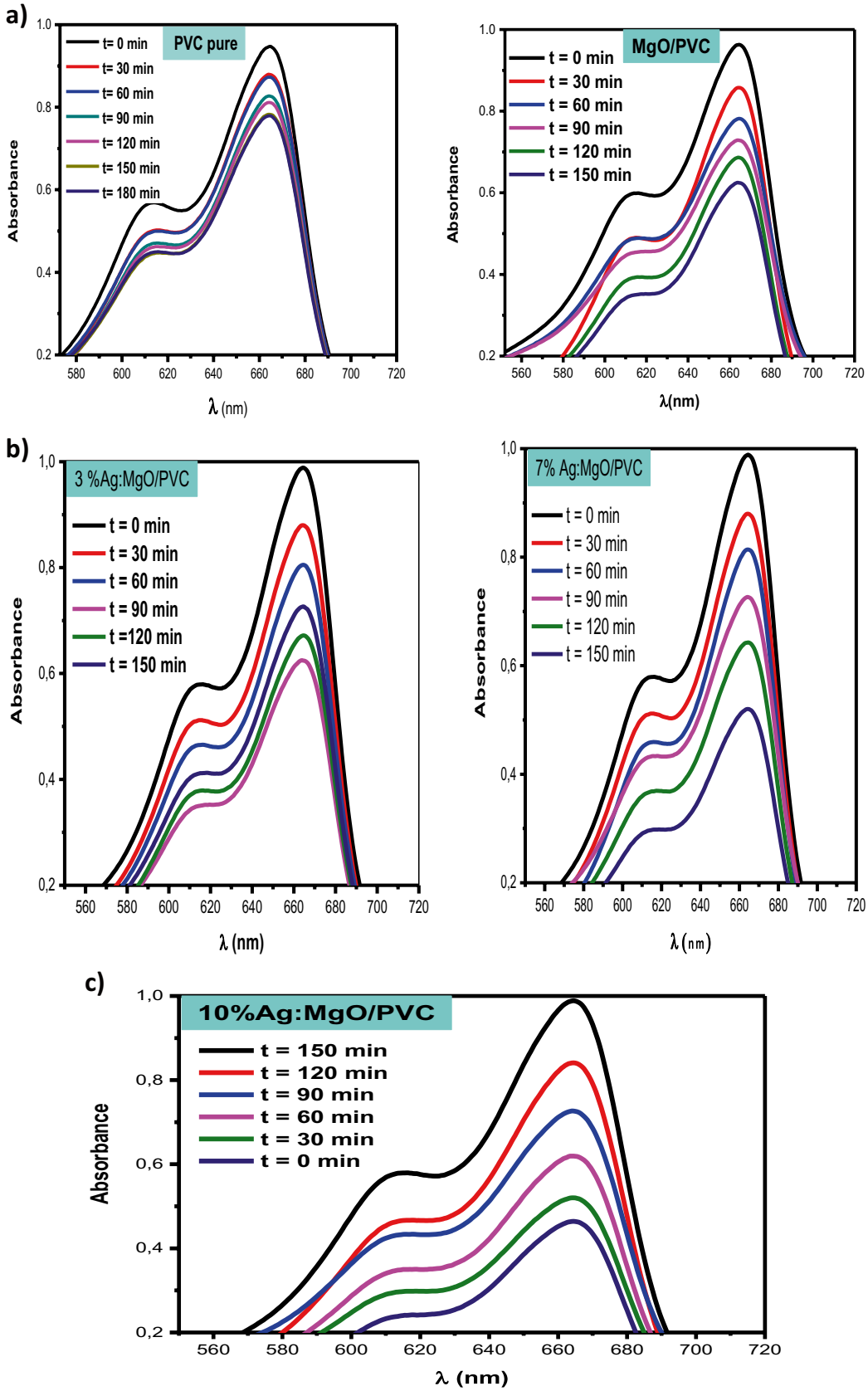

Fig. 6 **a** Photocatalytic degradation and **b** the plots ln (C_0/C) versus time; **c** degradation rate of MB dye under UV light irradiation of PVC; MgO/PVC and Ag:MgO/PVC nanocomposites thin films

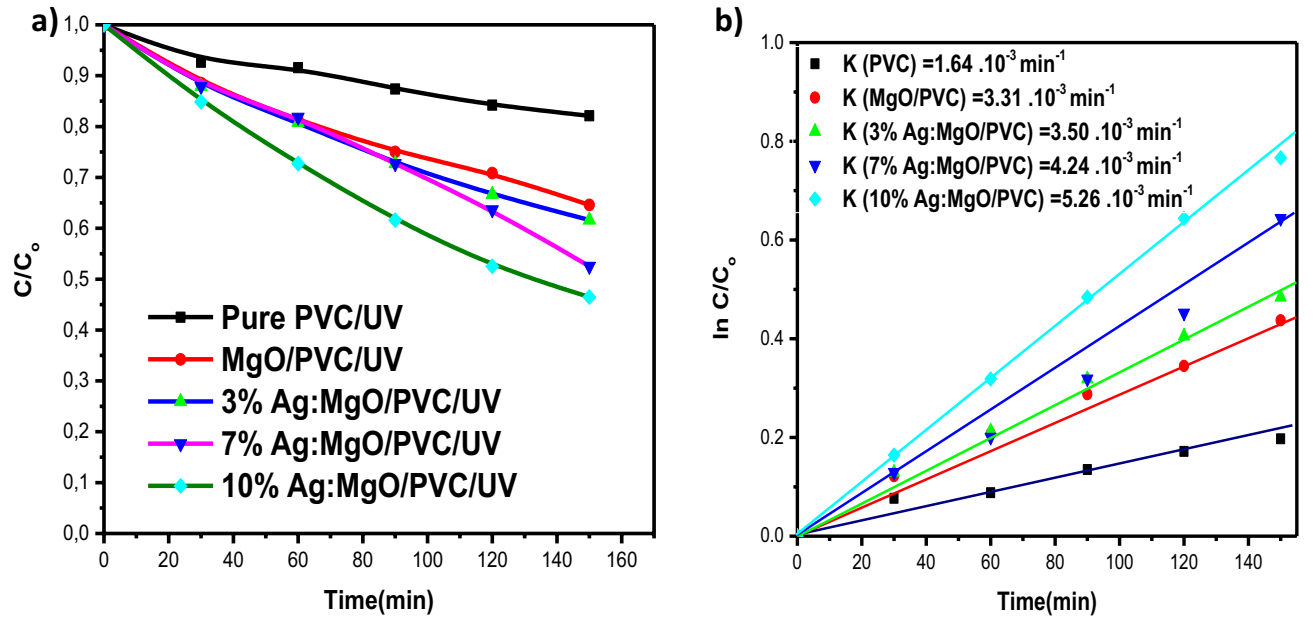

Fig. 7 Decomposition of the dyes (MB) under UV light **a** C/Co vs time **b** ln C/Co vs time **c** % dye degration vs time

The oxygen molecules (O_2) have an important central role in the degradation reactions of PVC matrix. Once the carbon-centered radicals included in the PVC polymer chain, their successive reactions lead to the chain cleavage with the O_2 incorporation and CO2 evolution.

$$-(\cdot CHCHCl) - +O_2 \rightarrow -(CH(OO\cdot)CHCl)- \quad (10)$$

$$-(CH(OO\cdot)CHCl) - + -(CH_2CHCl) \rightarrow -(CH(OOH)CHCl) - + -(\cdot CHCHCl)- \quad (11)$$

$$-(CH(OOH)CHCl) - +hu \rightarrow (CH(O\cdot)CHCI) - + \cdot OH \quad (12)$$

$$\cdot OH + MB\ Dye \rightarrow CO_2 + H_2O \quad (13)$$

Conclusion

A spin-coating approach was used used to deposit Ag:MgO/PVC nanocomposites films. A detailed investigation of optical, morphological and structural properties was also carried out. The investigations revealed by FTIR, XRD indicate Ag doped in MgO NPs. The studies also reveal a clear dispersion of Ag: MgO NPs in matrix of PVC. The increase in Ag: MgO content also enhanced the crystallinity and grain size. According to AFM we deduce that 7%, 10% Ag: MgO/PVC nanocomposites films are porous structure. Films of Ag: MgO/PVC nanocomposites are transparent and transmission optical band gap decrease from 4.1 eV to 3.69 eV. The application of Ag: MgO/PVC nanocomposites thin films was checked for photocatalysis. The improvement in photocatalytic activity was noticed for the degradation test of organic pollutants under UV light, Ag:MgO NPs enhanced photocatalytic efficiency of PVC film.

Acknowledgments Authors are thankful to the Researchers Supporting Project number (RSP-2021/132), King Saud University, Riyadh, Saudi Arabia

References

1. Jeon IY, Baek JB (2010) Nanocomposites Derived from Polymers and Inorganic Nanoparticles. J Mater. 3(6):3654–3674. https://doi.org/10.3390/ma3063654
2. Roy S, Srivastava SK, Mittal V (2016) Facile noncovalent assembly of MWCNT-LDH and CNF-LDHas reinforcing hybrid fillers in thermoplastic polyurethane/nitrilebutadiene rubber blends. J Polym Res 23:36. https://doi.org/10.1007/s10965-016-0926-4
3. Meti S, Bhat UK, Rahman MR (2020) Colossal dielectric permittivity of Nylon-6 matrix-based composites with nano-TiO2 fillers. Applied Physics A 126:264. https://doi.org/10.1007/s00339-020-3445-4
4. Agarwal S, Saraswat VK (2015) Structural and optical characterization of ZnO doped PC/PS blendnanocomposites. J Opt Mater. https://doi.org/10.1016/j.optmat.2015.01.024
5. Balakrishnan G, Velavan R, Batoo KM, Raslan EH (2020) Microstructure, optical and photocatalytic properties of MgO nanoparticles. https://doi.org/10.1016/j.rinp.2020.103013
6. Tang ZX, Lu BF (2014) MgO Nanoparticles as antibacterial agent: Preparation and Activity Brazilian. J Chem Eng 31:591–601. https://doi.org/10.1590/0104-6632.20140313s00002813
7. Cai Y, Wu Dan, Zhu X, Wang Wei, Tan Fatang, Chen J, Xueliang Q, Qiu X (2016) Sol-gel preparation of Ag-doped

MgOnanoparticles with high efficiency for bacterialinactivation. J Ceramics Int. https://doi.org/10.1016/j.ceramint.2016.10.041
8. Gulati U, Rajesh UC, Rawat DS, Zaleski JM (2012) Development of magnesium oxide-silver hybrid nanocatalysts for synergistic carbon dioxide activation to afford esters and Heterocycles at Ambient Pressure. J. N ame.00:1–3 .https://doi.org/10.1039/C9GC04040D
9. Yıldırım OA, Unalan HE, Durucan C (2013) Highly Efficient Room Temperature Synthesis of Silver-Doped Zinc Oxide(ZnO:Ag) Nanoparticles: Structural, Optical, and Photocatalytic Properties. J Am Ceram Soc 96(3) 766–773. https://doi.org/10.1111/jace.12218
10. Hosseini SM, Abdolhosseini I. Kameli SP, Salamati H (2015) Effect of Ag doping on structural, optical and photocatalytic properties of ZnO nanoparticles. J Alloys Compd 640:408–415 https://doi.org/10.1016/j.jallcom.2015.03.136
11. Feldman D (2014) Poly(vinyl chloride) Nanocomposites. J Macromol Sci, Part A: Pure Appl Chem 51:659–667. https://doi.org/10.1080/10601325.2014.925265
12. Chem TJ (2004) Turk J Chem 28:725–729
13. Deng Z, Zhu H, Deng Z, Zhu H, Peng B, Chen H, Sun Y, Gang X, Jin P, Wang J (2012) Synthesis of PS/Ag nanocomposite spheres with catalytic and antibacterial activities. J ACS Appl Mater Interfaces (4):5625−5632. https://doi.org/10.1021/am3015313
14. Zhou X (2015) Ag-doping improving the detection sensitivity of bolometer based on ZnO thin films. J Vacuum 117:47e49
15. Kang HS, Ahn BD, Kim JH, Kim GH, Lim SH, Chang HW, Lee SY (2006) Structural, electrical, and optical properties of p-type ZnO thin films with Ag dopant. Appl Phys Lett 88:202108
16. Li W, Kong C, Ruan H, Qin G, Huang G, Yang T, Liang W, Zhao Y, Meng X, Yu P (2012) Electrical properties and Raman scattering investigation of Ag doped ZnO thin films. Solid state communications 152:147–150
17. Cai Y, Wu D, Zhu X, Wang W, Tan F, Chen J, Qiao X, Qiu X (2017) Sol-gel preparation of Ag-doped MgO nanoparticles with high efficiency for bacterial inactivation. Ceram Int 43:1066–1072
18. Ahmad KS, Jaffri SB (2018) Phytosynthetic Ag doped ZnO nanoparticles: Semiconducting green remediators. J Open Chem 16:556–570. https://doi.org/10.1515/chem-2018-0060
19. Kassaee MZ, Mohammadkhani M, Akhavan A, Mohammadi R (2011) In situ formation of silver nanoparticles in PMMA via reduction of silver ions by butylated hydroxytoluene. Struc Chem 22:11–15
20. Vodnik VV, Vuković JV, Nedeljković JM (2009) Synthesis and characterization of silver—poly(methylmethacrylate) nanocomposites. Colloid Polym Sci 287:847–851
21. Kandulna R, Choudhary RB, Maji P (2017) Ag-doped ZnO reinforced polymeric Ag:Zno/PMMA nanocomposites as electron transporting layer for OLED application. J Inorg Organomet Polym. https://doi.org/10.1007/s10904-017-0639-0
22. Almontasser A, Parveen, Azam A (2019) Synthesis, Characterization and antibacterial activity of Magnesium Oxide (MgO) nanoparticles. J IOP Conf Ser: Mater Sci Eng (577):012051. https://doi.org/10.1088/1757-899X/577/1/012051
23. Krehula LK, Papic A,Krehula S, Gilja V, Foglar L, Hrnjak-Murgic Z (2016) Properties of UV protective films of poly(vinyl-chloride)/TiO2nanocomposites for food packaging. J Polym Bull. https://doi.org/10.1007/s00289-016-1782-4
24. Natarajan S, Kumari J, Lakshmi DS, Mathur A, Bhuvaneshwari M, Parashar A, Pulimi M, Chandrasekaran M, Mukherjee A (2015) Differences in antibacterial activity of PMMA/TiO2/Ag nanocomposite on individual dominant bacterial isolates from packaged drinking water, and their consortium under UVC and dark conditions. J Applied Surface Science. https://doi.org/10.1016/j.apsusc.2015.11.223
25. Bhavitha KB, Nair AK, Mariya H, Jose J, Mayeen A ,Kala MS, Saha A, Thomas S, Oluwafemi OS, Kalarikka N (2018) In-situ Dose dependent Gamma ray Irradiated Synthesis of PMMA-Ag nanocomposites films for multifunctional applications. New J of Chem (2018). https://doi.org/10.1039/C8NJ02684J
26. Cho S (2001) Wonyong Choi; Solid-phase photocatalytic degradation of PVC–TiO2 polymer composites. J Photochem Photobiol A 143:221–228
27. Yang C, Deng K, Peng T (2011) Ling Zan;Enhanced Solid-Phase Photocatalytic Degradation Activity of a Poly(vinyl chloride)-TiO2 Nanocomposite Film with Bismuth Oxyiodide. J Chem Eng Technol 34(6):886–892
28. Yang C, Gong C, Peng T, Deng K (2010) Ling Zan; High photocatalytic degradation activity of the polyvinyl chloride (PVC)–vitamin C (VC)–TiO2 nano-composite film. J Hazard Mater 178:15